Isı Bilimi ve Tekniği Dergisi, 44, 1, 191-205, 2024
J. of Thermal Science and Technology
©2024 TIBTD Printed in Turkey
ISSN 1300-3615
e-ISSN 2667-7725
https://doi.org/10.47480/isibted.1494481

EFFECTS OF PISTON COATING ON COMBUSTION STABILITY IN A CRDI DIESEL ENGINE RUN UNDER DUAL-FUEL MODE

Ali ŞANLI [*], İlker Turgut YILMAZ [**], Ali ÖZ[***]
* Maritime Higher Vocational School, Piri Reis University, 34940, Tuzla, İstanbul, Türkiye,
asanli@pirireis.edu.tr
**Department of Mechanical Engineering, Faculty of Technology, Marmara Uni., 34722, Maltepe, İstanbul, Türkiye,
ilker.yilmaz@marmara.edu.tr
*** Department of Automotive, Technical Sciences Vocational School, Burdur Mehmet Akif Ersoy Uni., Burdur,
alioz@mehmetakif.edu.tr

(Geliş Tarihi: 12.06.2023, Kabul Tarihi: 21.12.2023)

Abstract: Combustion stability in diesel engines is defined by cycle-to-cycle variations. In this study, effects of piston coating and engine load on cycle-to-cycle combustion behavior were investigated in a diesel engine operated on gaseous fuel mixture at different loads. Coated and uncoated piston tests under dual-fuel and single diesel modes were performed at three different loads including 50 Nm, 75 Nm, and 100 Nm at a constant speed of 1750 rpm. The piston bowls were coated by %8 yttria stabilized zirconia with the thickness of 0.4 mm. Dual-fuel mode is consisted of mixture of hydrogen enriched synthetic biogas, with the percentage of 80% CH_4, 10% CO_2, and 10% H_2. Main combustion parameters (cylinder pressure with crank angle, peak cylinder pressure (CP_{max}), peak pressure rise rate (PRR_{max}), indicated mean effective pressure (IMEP), CA10, CA50, CA90, and CA10-90 duration) were addressed in view of cyclic aspects. The results showed that the piston coating was comparatively more effective in reducing the coefficient of variation (COV) and standard deviation (SD) values of main combustion parameters, especially at low and medium loads. SD, frequency distribution, and COVs of CP_{max} and IMEP were quite better at a medium test load of 75 Nm. The piston coating also reduced COV of CP with crank angle under all tests. As increasing the engine load, cyclic samples of CP_{max} and PRR_{max} enhanced and advanced for both diesel and dual-fuel modes. By the piston coating and engine loads, Cyclic CA10 and CA50 variations were slightly affected whereas cyclic CA90 were tremendously changed. Therefore, CA10-90 period was importantly affected by piston coating and load. The highest relationship among the main combustion parameters was between CP_{max} and PRR_{max} for both piston cases. In dual-fuel mode, a strong relationship emerged between IMEP and CP_{max} at low load.
Keywords: Piston bowl coating, cycle-to-cycle variations, Common Rail Direct Injection (CRDI) diesel engine, biogas.

ÇİFT YAKITLA ÇALIŞTIRILAN BİR OHDE DIZEL MOTORDA YANMA KARARLILIĞI ÜZERİNE PİSTON KAPLAMANIN ETKİLERİ

Özet: Dizel motorlarda yanma kararlılığı çevrimden çevrime değişimlerle belirlenir. Bu çalışmada, farklı yükler altında gaz karışımlarıyla çalıştırılan bir dizel motorda çevrimden çevrime yanma davranışları üzerine piston kaplamanın ve motor yükünün etkileri araştırılmıştır. 1750 d/d'lık sabit bir devirde, çift-yakıt ve dizel çalışma şartlarında kaplamalı ve kaplamasız piston testleri 50, 75 ve 100 Nm'lik üç motor yükü altında yapılmıştır. Piston çanağı 0.4 mm kalınlıkta yttria stabilize zirkonya ile kaplanmıştır. Çift-yakıt modu %80 CH_4, %10 CO_2 ve %10 H_2 karışımdan oluşan hidrojenle zenginleştirilmiş sentetik biyogazdır. Ana yanma parametreleri (krank açısına göre silindir basıncı, pik silindir basıncı (P_{maks}), pik basınç artış oranı (BAO_{maks}), ortalama indike basınç (OIB), KA10, KA50, KA90 ve KA10-90 süresi) çevrimsel açıdan ele alınmıştır. Sonuçlar göstermektedir ki; piston kaplama ana yanma parametrelerinin çevrimsel değişim katsayısı (ÇDK) ve standart sapma (SS) değerlerini azaltmada, özellikle düşük ve orta yüklerde oldukça etkindir. SS, frekans dağılımı ve CP_{maks} ile OIB için ÇDK değerleri 75 Nm'lik orta yükte oldukça iyidir. Ayrıca, tüm yüklerde piston kaplama krank açısına göre silindir basıncının ÇDK değerlerini de azaltmıştır. Motor yükü artarken, dizel ve çift-yakıt çalışmalarında P_{maks} ve BAO_{maks} için çevrimsel değerler artış göstermiş ve daha erken oluşmuştur. Piston kaplama ve motor yüküyle, KA10 ve KA50 parametrelerinin çevrimsel değişimleri küçük mertebelerde iken KA90 parametresinin çevrimsel değişimleri önemli orandadır. Sonuçta, KA10-90 süresi piston kaplama ve motor yüküyle birlikte önemli oranda değişmiştir. Ana yanma parametreleri arasındaki en büyük ilişki her iki piston için P_{maks} ve BAO_{maks} arasında olmuştur. Çift-yakıt modunda, düşük yükte OIB ve Pmaks arasında güçlü bir ilişki ortaya çıkmıştır.
Anahtar kelimeler: Piston çanağı kaplama, çevrimsel değişimler, Ortak-hat direkt enjeksiyon (OHDE) dizel motor, biyogaz.

NOMENCLATURE

$\bar{x}$	Mean value
SD	Standard deviation
COV	Coefficient of variance
CRDI	Common rail direct injection
PRR_{max}	Maximum pressure rise rate [bar/°CA]
CP_{max}	Maximum cylinder pressure [bar]
IMEP	Indicated mean effective pressure [bar]
CA10	Crank angle when 10% of CHR emerged
CA50	Crank angle when 50% of CHR emerged
CA90	Crank angle when 90% of CHR emerged
CA10-90	Combustion duration [°CA]
R	Correlation coefficient
n	Cycle number
CH_4	Methane
H_2	Hydrogen
ESR	Energy substitution rate
LHV	Lower heating value [kJ/kg]
$\dot{m}$	Mass flow rate [kg/h]
YSZ	Yttria stabilized zirconia
TBC	Thermal barrier coating

INTRODUCTION

Internal combustion engines (ICEs) are frequently used for power producing, transportation, industrial applications, shipping propulsion, generators, and vehicles. Compression ignition (CI) engines are further preferred than spark ignition engines due to high efficiency, lower fuel consumption, and carbon-related emissions. About two-third of energy produced in ICEs is lost through coolant and exhaust systems. If heat loss through cooling is reduced, not only thermal efficiency can be increased, but also emissions can be reduced, and fuel economy improved (Hazar et al., 2016; Assanis et al., 1991).

Thermal barrier coating (TBC) of some engine components makes this possible by reducing the heat transfer from combustion chamber. Plasma spray method shows simple operation and high preparation efficiency, therefore used in most TBC applications. In ICE applications, TBC is applied to engine components such as pistons, valves, cylinder heads and exhaust manifolds that are exposed to high-temperature combustion gases in ICEs. Coated engine parts become more resistant to wear, friction, heating, corrosion, and oxidation. TBC system usually consist of two layers: bond and main coat materials. The first is the bond layer, which protects the substrate against oxidation and corrosion and also ensures compatibility between the ceramic layer and the substrate. The latter, with low thermal conductivity, greatly reduces heat losses to surrounding sources. TBC helped to extend the life of components in aircraft engines and stationary gas turbines by reducing the metal temperature (Schulz et al., 2003). The high combustion temperature resulting from the thermal insulation of ICE components can result in relatively higher thermal efficiency and lower fuel consumption (Taymaz, 2007; Selvam et al., 2018). Thanks to the thermal insulation of the exhaust manifold, the heat carried by the exhaust gases can also be used to further drive the turbocharger turbine, which increases volumetric efficiency and improves engine performance (Godiganur, 2021). Reducing carbon dioxide (CO_2) and hydrocarbon (HC) emissions, and improvement in aftertreatment performance by accelerating the catalyst light-off time can be possible with the thermal insulation of combustion chamber parts. Coating the walls of the combustion chamber with materials with lower thermal conductivity has been practiced since the 80s, but the results have not always been satisfactory (Vittal et al., 1999). It is needed to durable engine parts to resist higher temperatures caused by TBC. On the other hand, the increase in NO_x emissions is high due to such high combustion temperatures in the TBC engine (Hazar, 2010; Reddy et al., 2021; Aydın, 2013). It is possible to reduce NO_x emissions by using the internal exhaust gas recirculation (Shabir et al., 2014) or alternative fuels (Özer et al., 2021). All of them has partly prevented TBC technology from becoming widespread.

Numerous materials such as yttria stabilized zirconia (YSZ), silicon carbide, titanium, mullite, anodized alumina, magnesium silicate, molybdenum can be used for insulating the parts of combustion chamber in ICEs. Research groups in academic environment are still studying to obtain reasonable results by means of coating the engine parts. The effects of piston coating with different thicknesses of YSZ on the performance of different CI engines were investigated (Selvam et al., 2014; Sivakumar and Kumar, 2014; Goud et al., 2015). Coating process was done by the plasma spray method, and the used material had acceptable properties in view of lower thermal conductivity, higher thermal expansion coefficient, stable phase structure, and high Poission's ratio at elevated temperatures. Better thermal efficiency, lower fuel consumption, and lower HC and CO emissions were obtained in the engine with coated piston compared to the standard engine. Temperature on the coated piston was higher than that on the uncoated piston, and thickness of the coating material on the piston was highly important in view of temperature and thermal stress distribution (Cerit and Coban, 2014). Hejwowski and Weronski (2002) performed an experimental and simulation study in a naturally aspirated CI engine used different coating materials on the piston crown, which were ZrO_2, Al_2O_3, and TiO_2. Engine power and torque respectively enhanced almost 8% and 6%, and brake specific fuel consumption (bsfc) decreased about 15-20% by the coated piston. Simulation findings demonstrated that the optimum thickness of the coating material on piston was below 0.5 mm, and the coating material with aluminum-titania had the strongest corrosion resistance. Ramasamy et al. (2021) compared the coating materials on the piston of a CI engine fueled with diesel and biodiesel. They emerged that the YSZ material gave better results concerning the engine performance, whereas $Al_2O_3.SiO_2$ material showed lower emissions of NO, CO_2, and CO for each fuel type. Similarly, Ali et al.

(2018) performed a numerical comparative study on the effects of different ceramic materials (YSZ and TiO_2) applied on the piston surface on the performance of dual-fuel engine. YSZ revealed promising results compared to TiO_2, which had higher indicated thermal efficiency, lower bsfc, and higher exhaust gas temperature. Aydın et al. (2015) carried out performance, emission and combustion investigations in biomass fueled CI engine whose piston and valves were coated with ZrO_2, MgO, and Al_2O_3 materials. TBC improved bsfc and thermal efficiency results. NO_x emissions partially elevated but HC, CO, and smoke emissions reduced with TBC application. Cylinder pressure relatively enhanced for the engine with coating parts. Civiniz et al. (2008) reported a 2% increase in engine power, and 1.5-2.5% increase in engine torque, and 4.5-9% reduction in bsfc by coating the piston, cylinder head, and valves of the test engine. The NO_x emissions enhanced by 10%, and the smoke emission decreased by about 18% with the TBC application. Experimental results with the piston coating application can sometimes reveal contrary results to the expected ones; for instance, lower indicated thermal efficiency and higher soot values could be observed at partial loads (Caputo et al., 2019), higher bsfc values (Serrano et al. 2015), and lower NO_x emissions (Ramu et al. 2009; Lawrence et al. 2011).

Cyclic variations directly influence the engine performance, emissions, combustion stability and engine noise. Drivability viewpoint of the vehicles with a multi cylinder engine might be closely related to cyclic combustion variability. Residuals from previous cycle, variations of air/fuel ratio, ignition delay, fuel type, and fluctuations in pressure, timing, and duration of fuel injection are usually responsible to the cycle-to-cycle variabilities. In the literature, there are several studies on alternative fuels in diesel engines (Şanlı, 2023; Kyrtatos et al. 2016; Pera et al., 2013, Wang et al., 2015; Zhong et al., 2003; Adomeit et al., 2007; Barton et al., 1970; Gupta et al., 2019). The overall conclusion from the studies is that cycle-to-cycle combustion variations are very important as they limit the load and power range in dual-fuel mode.

In most of the published papers, performance and emission analysis of the engine running on alternative fuels have been performed. Effects of TBC on combustion stability of the diesel engines working with the alternative fuels are seen unclear therefore it is needed more detailed investigations. This study was carried out to gain an in-depth understanding of the combustion behavior of a dual-fuel diesel engine with the coated piston bowls. The study is novel and fills the gap in the literature on cycle-to-cycle variations of the piston-coated dual-fuel diesel engines. Comprehensive cyclic combustion results are presented and discussed in this study for the coated and uncoated pistons under diesel and dual-fuel modes at different loads for the CRDI diesel engine.

EXPERIMENTAL METHOD

Test Equipment

Experiments were performed in a four-cylinder, Renault K9K, CRDI diesel engine to investigate cyclic variability under gaseous fuel operation. Diesel fuel having euro-diesel norms was used in the tests. Engine exhaust gas recirculation valve was canceled to avoid the partial effects of the exhaust gases. Before the tests, the engine was idled for a while to reach a stable regime. For the investigation, test conditions at which the engine was mostly operated under normal driving conditions were selected. The tests were performed at three loads, covering 50, 75, and 100 Nm torques. Engine speed was kept constant at 1750 rpm. The engine properties are given in Table 1, and Fig. 1 presents test bench layout. An eddy-current dynamometer, measurement capable of 150 kW rated power and 8000 rpm maximum rotational speed, was used to adjust the load and speed variations of the test engine. K-type thermocouples measured temperature variations at critical points of the engine, such as inlet and outlet cooling water, lubrication oil, exhaust gas outlet and fuel inlet. Measurement of the air mass flow rate was done by New Flow air flow meter. Instantaneous cylinder pressure data were collected by Optrand glow plug type cylinder pressure sensor. 200 sequential pressure data were used for the investigation. A shaft encoder with a resolution of 1° detected the crank angle degree. Instantaneous fuel pressure was metered by Kistler model fuel pressure device and its data were amplified by a Kistler charge amplifier. Amplified pressure signal was passed on National Instrument data card and send into a computer for combustion analysis. An on-board diagnostic device (OBD) was connected to the engine electronic control unit in order to show numeric data from the chosen engine sensors.

Table 1. Engine specifications

Main properties	Four-stroke, turbocharger, CRDI fuel injection system
Number of cylinders	4
Bore - Stroke	76 mm - 80.5 mm
Compression ratio	18.25:1
Total stroke volume	1.461 liter
Injector type	With 5 nozzle holes, Selenoid controlling by Delphi management system
Maximal torque (@1750 rpm)	160 Nm
Maximal power (@4000 rpm)	48 kW

.

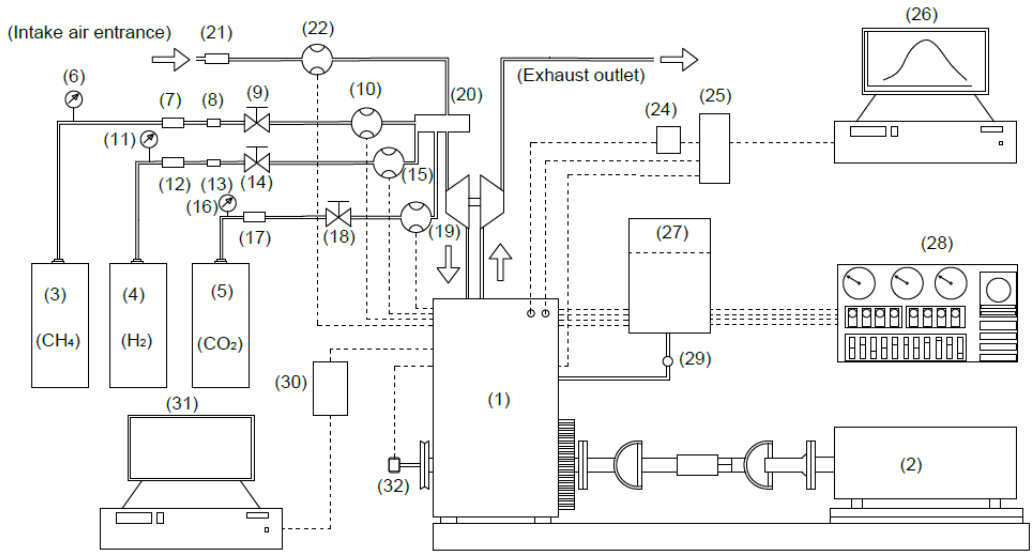

1.Test engine, 2.Eddy-current dynamometer, 3.CH4 tube, 4. H2 tube, 5. CO2 tube, 6-11-16.Manometers, 7-12-17. Pressure regulators, 8-13.Flame arresters, 9-14-18.Control valves, 10-15-19. Gas flow meters, 20.Mixing chamber, 21.Air filter, 22. Air flow meter, 23. Exhaust , 24.Charge amplifier, 25. Data card, 26. PC for combustion and emissions data, 27.Diesel tank, 28.Dynamometer control, 29. Burette, 30. On board diagnostics card, 31. PC for OBD interface, 32. Crank shaft encoder.

Fig. 1. Test bench.

The gaseous fuels were supplied with 50-liter bottles and connected to the test system via appropriate tools. They were sent to a mixing room mounted on the intake line, and after the turbocharging process, the mixture of air-gaseous fuels was sent to the engine cylinders. The mixture was ignited by the conventional diesel (pilot fuel). Energy amount of the pilot diesel fuel was varied depending on the test conditions and adjusted in approximately 20% of the total energy amount. Flame arresters on CH_4 and H_2 gas lines were utilized to prevent back flow of the sparked gaseous fuel and a possible explosion. CH_4, CO_2, and H_2 flow rates were determined by Sierra model gas flow meters. In tests, entire metering values were displayed on the dynamometer control panel and OBD connected computer. Uncertainty of the used equipment is given in Table 2. After the standard engine tests, the standard pistons were replaced with YSZ-coated pistons. A similar test procedure was followed for the engine with the coated pistons.

In this study, the engine pistons were coated by YSZ and Ni-Al bond coat by plasma spray method. The coated and standard pistons can be seen in Fig. 2. 0.4 mm thicken YSZ surface ceramic coating (8%) and 0.1 mm thicken nickel-aluminum (Ni-Al) bond were applied to the piston bowl, respectively.

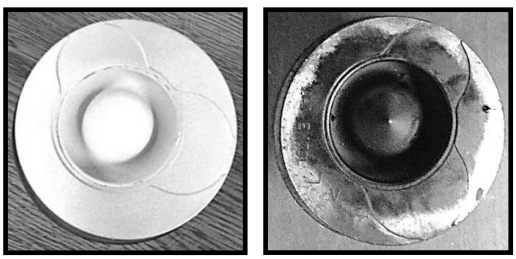

Fig. 2. Coated and standard pistons.

Calculation Method of Cycle-To-Cycle Analysis

Energy substitution rate (ESR) of each fuel was calculated by Eq. (1) presented below (Bouguessa et al., 2020),

$$ESR_{fuel} = \frac{\dot{m}_{fuel} LHV_{fuel}}{\dot{m}_d LHV_d + \dot{m}_{CH} + LHV_{CH4} + \dot{m}_{H2} LHV_{H2}} \quad (1)$$

where, $\dot{m}$ and LHV symbolize mass flow rate (kg/h) and lower heating value (kJ/kg) of the test fuels, respectively. ESR value of each fuel for the test cases are given in Table. 3. Combustion stability is defined by means of SD and COV. SD for examined combustion characteristic can be calculated from Eq. (2)

$$\mathrm{SD} = \sqrt{\frac{\sum_{i=1}^{n}(X_i - \bar{X})^2}{n-1}} \quad (2)$$

where $\bar{X}$ and X_i express mean value and parameter value at cycle number i of a combustion parameter, respectively. n represents number of the cycles, which is 200 in this study.

COV calculation of the combustion parameters is shown in Eq. (3), as follows:

$$COV = \frac{\mathrm{SD}}{\bar{X}} 100\% = \frac{\sqrt{\frac{\sum_{i=1}^{n}(X_i - \bar{X})^2}{n-1}}}{\bar{X}} 100\% \quad (3)$$

In this paper, relationships among CP_{max}, PRR_{max}, and IMEP parameters were addressed. Correlation coefficient R reveals numerical relationship between two combustion findings, referred as X and Y, and is computed from Eq. (4) (Şanlı et al. 2020),

$$R(X,Y) = \frac{\frac{1}{n}[\sum_{i=1}^{n}(X_i-\bar{X})(Y_i-\bar{Y})]}{\mathrm{SD}_{(X)}\mathrm{SD}_{(Y)}} \quad (4)$$

Table 2. Properties of the test apparatus.

Parameter	Unit	Measurement range	Accuracy
Fuel line pressure	bar	0 ~ 3000	0.5 %
Cylinder pressure	bar	0 ~ 200	1%
CH_4 flow rate	l/min	max. 200	1%
H_2 flow rate	l/min	max. 200	1%
Air flow rate	m^3/h	max. 1200	1%

Table 3. Energy substitution rates of dual-fuel diesel modes under different loads and pistons.

Load (Nm)	Standard piston			Coated piston		
	Diesel (%)	CH_4 (%)	H_2 (%)	Diesel (%)	CH_4 (%)	H_2 (%)
50	23	74.6	2.4	19.8	77.5	2.7
75	22	75.5	2.5	21	76.2	2.8
100	23	74.6	2.4	20	77.4	2.6

RESULTS AND DISCUSSION

Cyclic Cylinder Pressure Variations

Under the dual-fuel and single diesel operations, cyclic cylinder pressure traces versus crank angle for the 200 sequential cycles are shown in Fig. 3 and Fig. 4 for YSZ coated piston and standard piston operations. It is observed from the figures that the cylinder pressure fluctuations for all cases are generally stable. The coated piston significantly affected magnitude of the cylinder pressure. This is clearly recognized in Fig. 5. Moreover, SD and COV of CP at each crank angle are presented in Fig.5. First of all, trend of COV of CP well agrees with published literature (Liu et al., 2022). Trend of COV of CP emerged that the coated piston at 100 Nm caused to strength pressure oscillations under dual-fuel modes, and peak COV of CP was reduced with the piston coating as well as lower COV values of 3%, suggesting the combustion stability was smoother in case of the coated piston. Fig. 6 is presented for a detailed examination of the cycle-to-cycle variations of CP_{max}. Additionally, average, SD, COV values, and frequency distribution of CP_{max} are indicated in the Fig.6. Compared to the standard piston, the average value of the CP_{max} for the coated piston under dual-fuel mode increased from 86.83 bar to 95.65 bar at 50 Nm, from 101.48 bar to 125.18 bar at 75 Nm, and from 133.26 bar to 137.02 bar at 100 Nm load. Apparent elevation of CP_{max} was valid for the coated piston under the single diesel operation. This can be attributed to less heat loss to the cylinder walls and higher cylinder gas temperature caused from the piston coating (Yao et al., 2018). SD reflects the deviation from the mean value. Its minimum value is generally preferred for any variable. Generally, a lower SD value was found with coated piston at tested engine loads. COV presents the degree of dispersion of data samples around the mean. COV of CP_{max} was mostly lower with the coated piston operations. It varies similarly to the SD of CP_{max}.

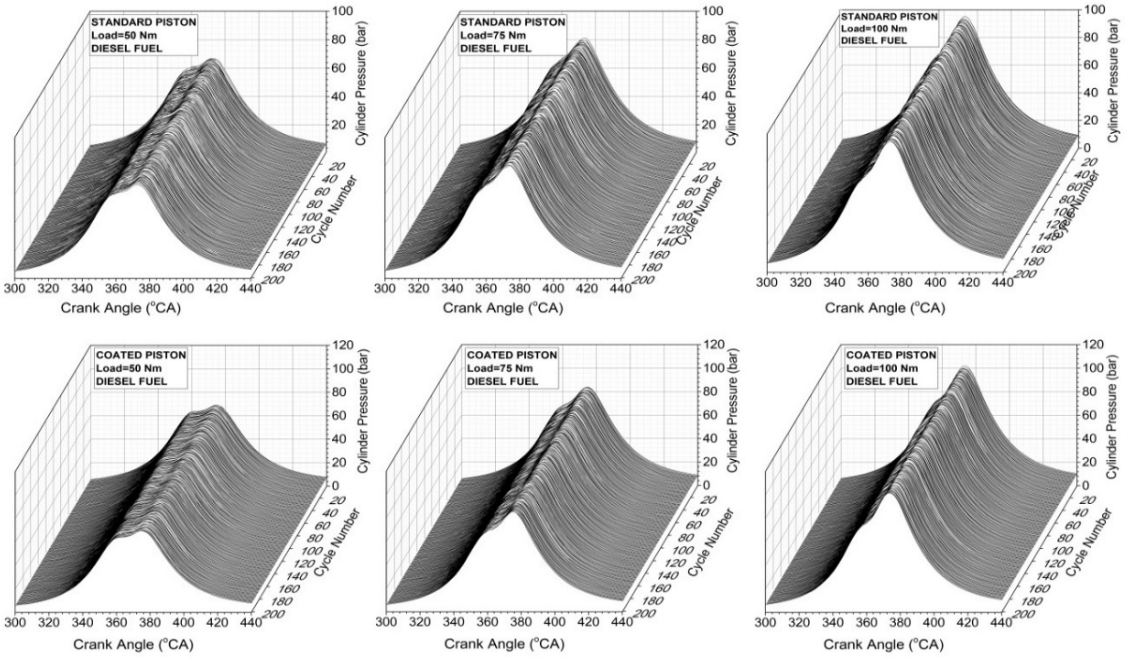

Fig. 3. Cyclic cylinder pressure curves with crank angle for standard piston and coated piston at different loads under single diesel mode.

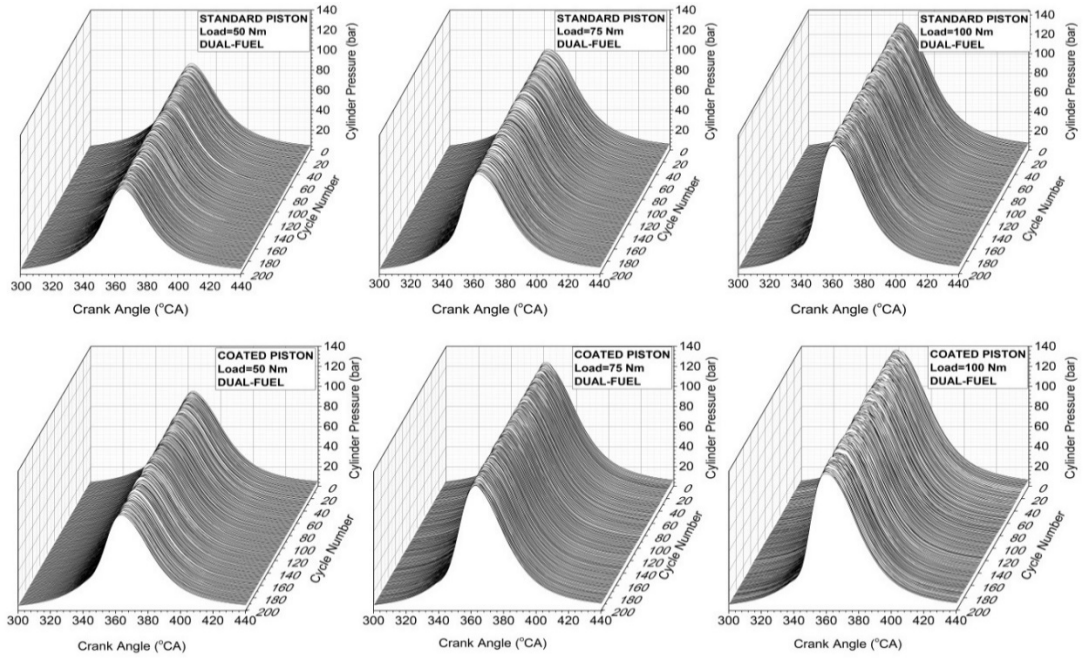

Fig. 4. Cyclic cylinder pressure curves with crank angle for standard piston and coated piston at different loads under dual-fuel mode.

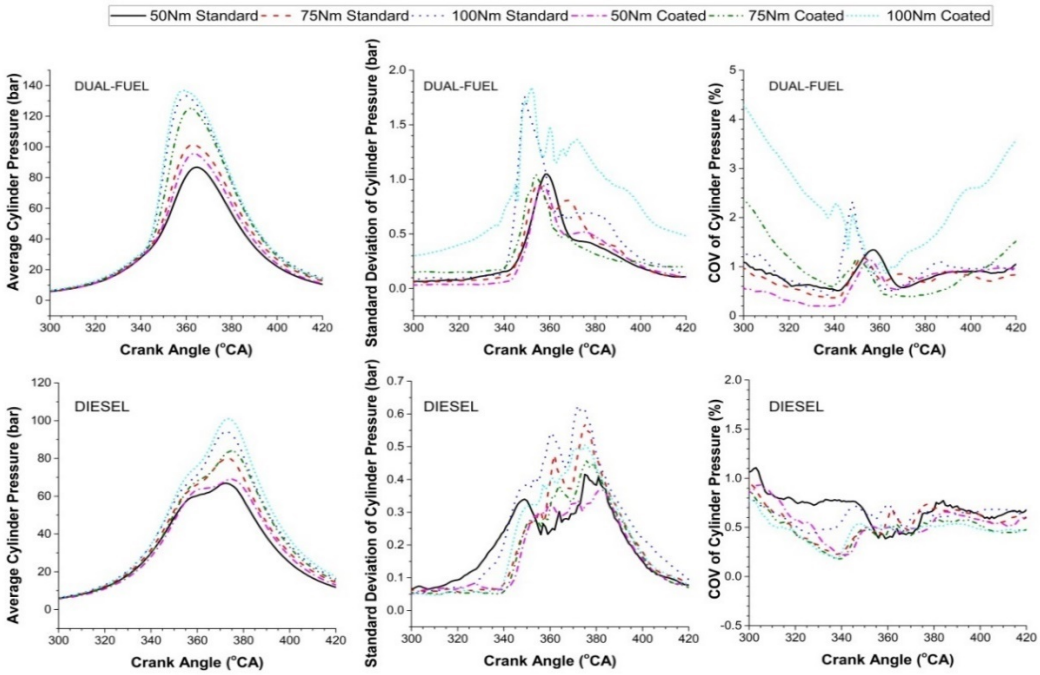

Fig. 5. Average, SD, and COV of cylinder pressure with crank angle for coated and standard piston engine at different engine loads under diesel and dual-fuel mode.

Frequency distribution reflects the repeatability for the same value of any parameter. A larger number of frequency distributions means more repeatability for the same value during multi-cycles. It can be clearly seen that the maximum frequency of CP_{max} occurs at 50 Nm load in diesel mode and 75 Nm load in dual-fuel mode, regardless of whether the pistons are coated or uncoated. It was observed that under 100 Nm load, the frequency distribution of CP_{max} was wider, i.e. more CP_{max} values occurred, so a larger variety of CP_{max} values emerged.

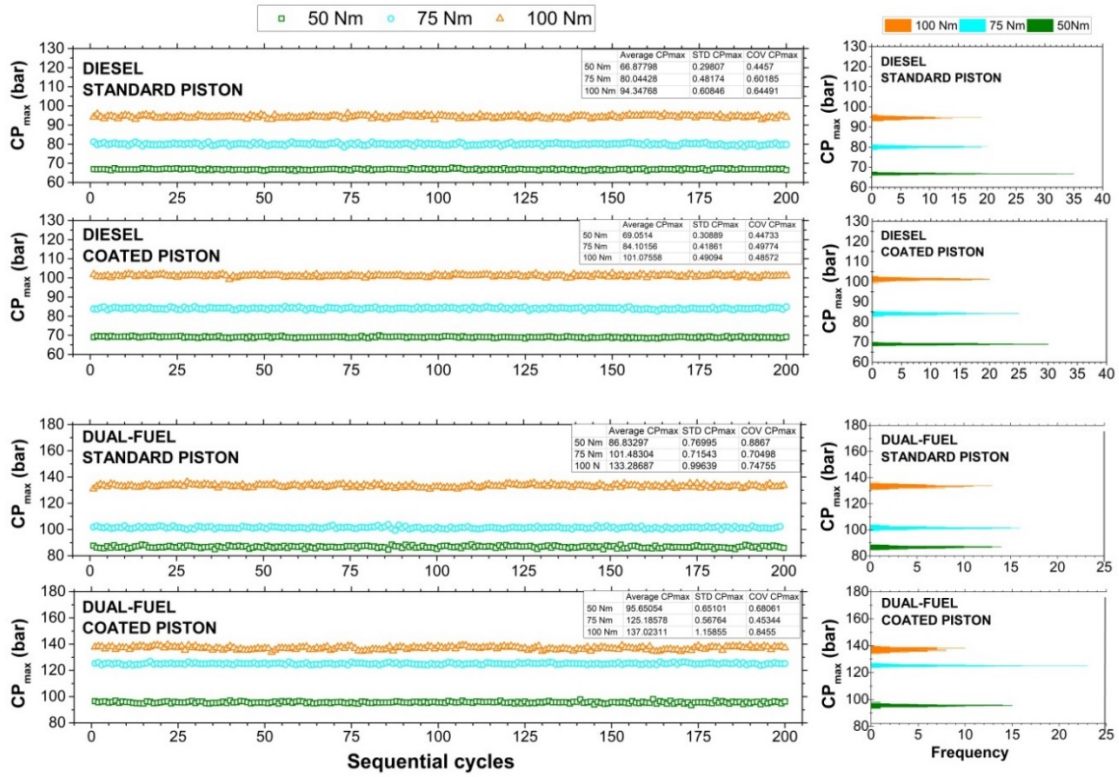

Fig. 6. Cyclic CP_{max} and frequency variations for standard and coated pistons at various fuel and load cases.

CP_{max} values and their crank angle (CA) locations are presented in Fig. 7 for all test conditions. As the load was increased the cyclic CP_{max} locations notably advanced under dual-fuel mode; whereas it slightly advanced under single diesel mode. It can be hence said that CP_{max} locations are more sensitive to load changing in operation with the gaseous fuels. In the case of coated piston, earlier CP_{max} positions were observed in dual-fuel mode and later CP_{max} positions were observed in single diesel mode. The piston bowl coating keeps the heat energy of fuel in combustion chamber thus increasing the temperature of the burning gases in cylinders (Yao et al., 2018). The ignition points occur earlier in the piston bowl, especially with the gaseous fuel operations. Turbocharged diesel engines run with extremely lean air/fuel mixture at idle. Increased load means more fuel entering the cylinders; as a result, the combustion temperature increases. Especially, dual-fuel mode presents homogeneously operation all over the cylinders and is easily ignited by the pre-injection of the diesel fuel. The pre-injection timing is strongly dependent on the engine operating characteristics, especially the load variation, which is considered as a root cause of earlier CP_{max} locations (Wang et al., 2021).

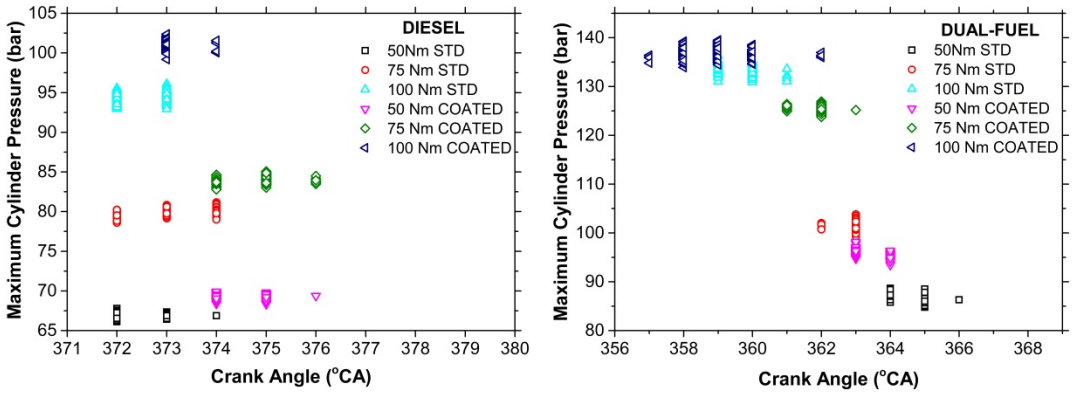

Fig. 7. CP_{max} and corresponding CAs at different cases.

Cyclic Pressure Rise Rate Variations

Pressure rise rate (PRR) is a meaningful tool for evaluating the knock during the burning phase. Cyclic variations of the PRR during 200 cycles are seen in Fig. 8 for different cases. As increasing the engine load, it can be clearly observed that cyclic PRR_{max} values elevate for each test case. Average PRR_{max} was detected as 3.91,

5.69, and 9.59 bar/°CA at 50 Nm, 75 Nm and 100 Nm loads respectively for the standard piston operation of dual-fuel mode, while 5.01, 7.99, and 10.6 bar/°CA at 50 Nm, 75 Nm and 100 Nm loads respectively for the coated piston operation in dual-fuel mode. Remarkable PRR_{max} increase was not detected for single diesel mode. From these observations, it can be concluded that the coating piston significantly affected the cyclic PRR_{max} values. At high load of 100 Nm and piston coating caused to the severe diesel knock with the high average value of 10.6 bar/°CA. Some cycles led to higher PRR_{max} values at 100 Nm under dual-fuel coated piston mode. The highest PRR_{max} value happened in 65. cycle with a value of 12.15 bar/°CA at the stated test case.

Frequency distribution of PRR_{max} showed that the dual-fuel mode led to extremely lessen the repeatability of PRR_{max} values. The highest value of PRR_{max} frequency in single diesel mode was 63 at 50 Nm under uncoated piston and 59 times at 75 Nm under coated piston. The highest frequency value of PRR_{max} in dual-fuel mode was 17 at 75 Nm under uncoated piston and 16 at 75 Nm under coated piston. On the other hand, the load increasing was resulted in more PRR_{max} values and therefore less PRR_{max} frequency. Higher temperatures and severe pressure oscillations caused by the increase in the amount of fuel delivered into the cylinders and ignition cores due to increasing the engine load can be among possible reasons for the higher frequency of PRR_{max} values. Similarly, the coating of piston bowl mostly led to an increase in frequency distribution of PRR_{max}; in other words, the repeatability of the same values increased. Sometimes, this may be associated with the SD variations. In all tests, COV of PRR_{max} values were lower than 3%. This means that the stable running was continued during the tests. When the engine was operated with the coated piston, remarkable decrease in COV of PRR_{max} was seen, especially in dual-fuel mode. For example, when the engine's standard pistons were replaced with the coated ones, COV of PRR_{max} at 75 Nm load dropped from 2.18 bar/°CA to 1.90 bar/°CA in dual-fuel mode. Moreover, the lowest COV of PRR_{max} values was obtained at 75 Nm. This indicates that the test engine operates the best at that load in view of the cyclic variations.

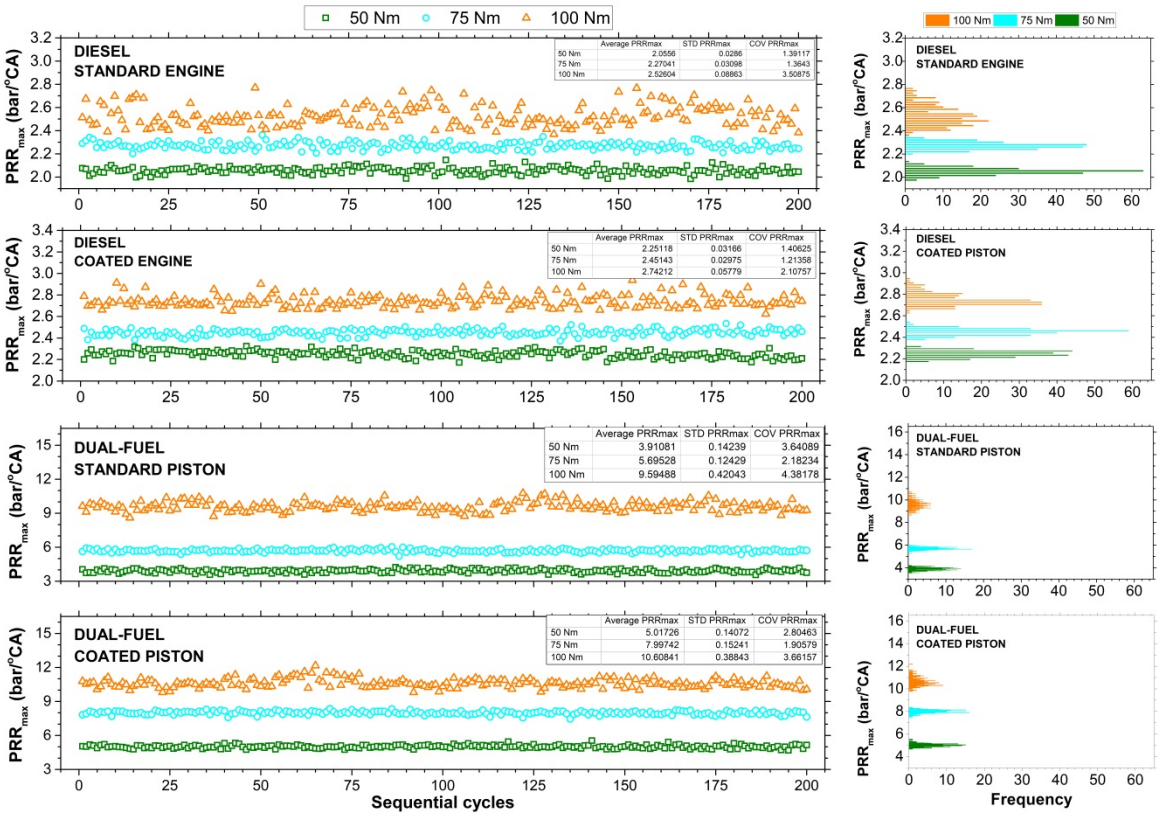

Fig. 8. Cyclic PRR_{max} and frequency variations for standard and coated pistons at various fuel and load cases.

PRR_{max} values and its corresponding crank angle positions for 200 experimental samples are illustrated in Fig. 9 for different cases of the fuels, loads and coatings. Mostly, a similar trend to the CP_{max} outcomes was observed under the diesel and dual-fuel modes. As the engine load was enhanced, advanced CA locations and higher values of PRR_{max} were noticed. Compared to 50 Nm and 75 Nm loads, there were seen two CA groups of PRR_{max} locations for the conventional diesel operation at 100 Nm regardless of the coated or uncoated piston cases. This is due to the pre-injection and main injection phases of the common-rail fuel-injection system (Şanlı and Yılmaz, 2022). As changing the injection amount and timing with the engine load, first peak and second peak are more noticeable under sole diesel operations. On the other hand, the bowl coating caused to earlier CAs of

PRR_{max} at a given load. Increased temperatures and cylinder pressure oscillations with the engine load and the piston coating appear to promote severe diesel knocking. Besides, when the engine was operated in dual-fuel mode, PRR_{max} locations were notably retarded, in the range of 2-9 °CA at 50 Nm, 1-7 °CA at 75 Nm, and 2-6 °CA at 100 Nm. This can be ascribed to the dynamic injection timing variations, which is one of the superior specifications of the common-rail engine management system.

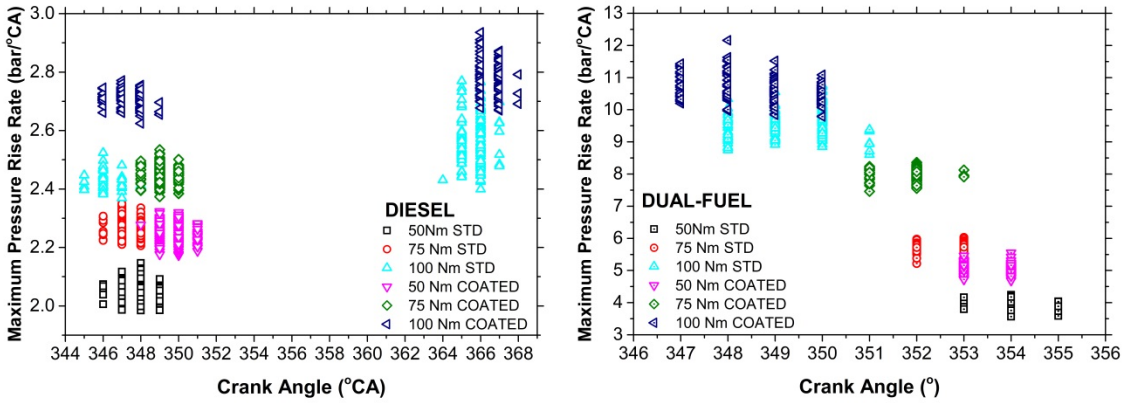

Fig. 9. Crank angle and PRR_{max} for coated and standard piston cases at different loads.

Cyclic IMEP Variations

IMEP reflects average cycle efficiency obtained by the indicator diagram. Sequential IMEP variations and frequency distribution for different test cases are illustrated in Fig. 10. It can be clearly observed that the cyclic IMEP values increase as the engine load increases. However, under dual-fuel mode and coated piston case of 100 Nm, the cyclic IMEP values were not enhanced more and remained similar to those of medium load. Average values were 8.76 bar and 8.74 bar for the respective loads of 75 Nm and 100 Nm in that test condition. Combined effects of the coated piston and high load under dual-fuel mode caused severe diesel knock as observed earlier in Figs. 8 and 9, and this apparently limited IMEP boost with enhanced load. In the published paper, Ramu and Saravanan (2009) reported lower IMEP values of TBC engine with fuel additive compared to uncoated engine. They emphasized that to be caused by lower power production during combustion process in TBC engine.

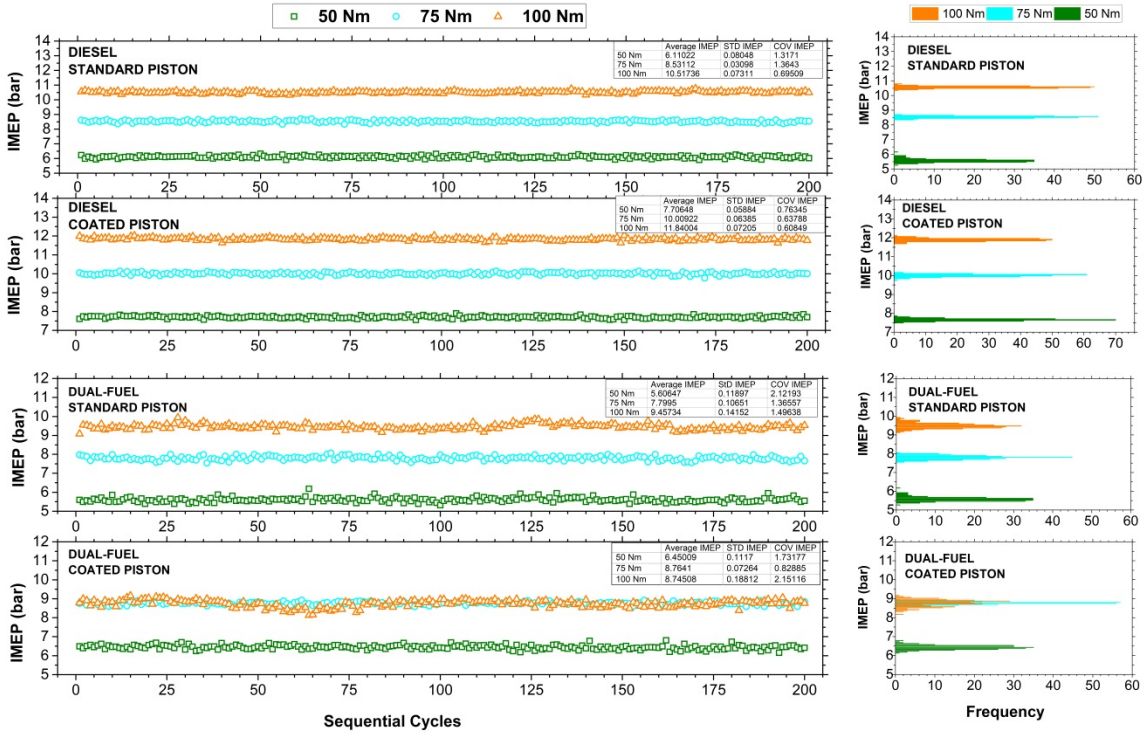

Fig. 10. Cyclic IMEP variations for standard piston and coated piston at various loads.

Cyclic CA10, CA50, CA90, and CA10-90 Variations

CA positions detected by corresponding cumulative heat release (CHR) findings are frequently used in combustion studies. The positions of CA10, CA50, and CA90 are important findings accounting for determining of the combustion phases. CA10, CA50, and CA90 are CA positions corresponding to 10%, 50% and 90% of the energy released by the combustion of each fuel respectively (Şanlı et al. 2020). They depend on engine design, fuel type, and load conditions. The positions of CAs during the combustion can be affected by several parameters such as intake conditions, injection characteristics, and ignition delay period. CA10-90 term describes the period from 10% to 90% of the burned fuel mass. Longer CA10-90 period clearly refers to slower combustion period, suggesting that more heat loss, inefficient combustion, lower thermal efficiency and power output, and more HC formation. In Figs. 11 and 12, CA10, CA50, CA90, and CA10-90 variations from one cycle to another are exhibited for all test cases. Cyclic CA10 and CA50 results at all tests showed modest differences. However, cyclic CA90 results exhibited larger oscillations during the sequential cycles. Cyclic CA10-90 variations therefore showed extreme fluctuations, indicating that the combustion duration in a cycle is greatly dependent on post-burning phase (Liu et al., 2022). It is perceived from the Figs. 11 and 12 that as the engine load was enhanced, cyclic CA90 and CA10-90 variations notably decreased in diesel fuel mode whereas increased in dual-fuel mode. At the end of the diffusion combustion, combined effects of the residual gases from the previous cycle and the unburned fuel in crevice regions play a critical role in cyclic fluctuations of CA90 and CA10-90 parameters. Furthermore, the cycle-to-cycle variation of the intake air pressure can be critical for the formation of CA points during the combustion phase. This is obviously proved in Fig. 13 for several subsequent cycles (cycle number from 147 to 151) in dual-fuel coated piston mode under 100 Nm load. In 148.-150. cycles, it was noticeable that the intake air was taken into the cylinders with relatively lower intake pressure compared to 147. and 151. cycles. During the post-combustion period, as seen in CHR graphic at right-hand below, it was detected later CA90 points in 148.-150. cycles. In the meantime, fuel line pressure graphic for the specified cycles, at left-hand above in Fig. 13, showed that the CA points were influenced by the injection pressure. It is obvious that similar injection pressure traces in 148. and 149. cycles yielded similar HRR and CHR profiles whereas no similar cylinder pressure profiles. Therefore, combined effects of the fuel injection pressure and the intake air pressure are proved to be quite effective in cycle-to-cycle combustion variations in this study. Moreover, it is clear from the Fig. 13 that as passing from CA10 to CA90, the crank interval between the CAs drastically enlarged. Additionally, when the coated piston was applied to the engine, it was observed cyclic improvement for CA90 and CA10-90 for each fuel mode. This is possibly due to improvement in the post-burning phenomenon and a reduction in the amount of the unburned gases in operation with the coated piston. In dual-fuel operation, combustion changes from a constant pressure process to a constant volume process. Overall, cyclic variations of examined CAs and CA10-90 period showed quite smooth variations compared to those in spark ignition engines in published literature (Liu et al., 2022; Chen et al., 2021).

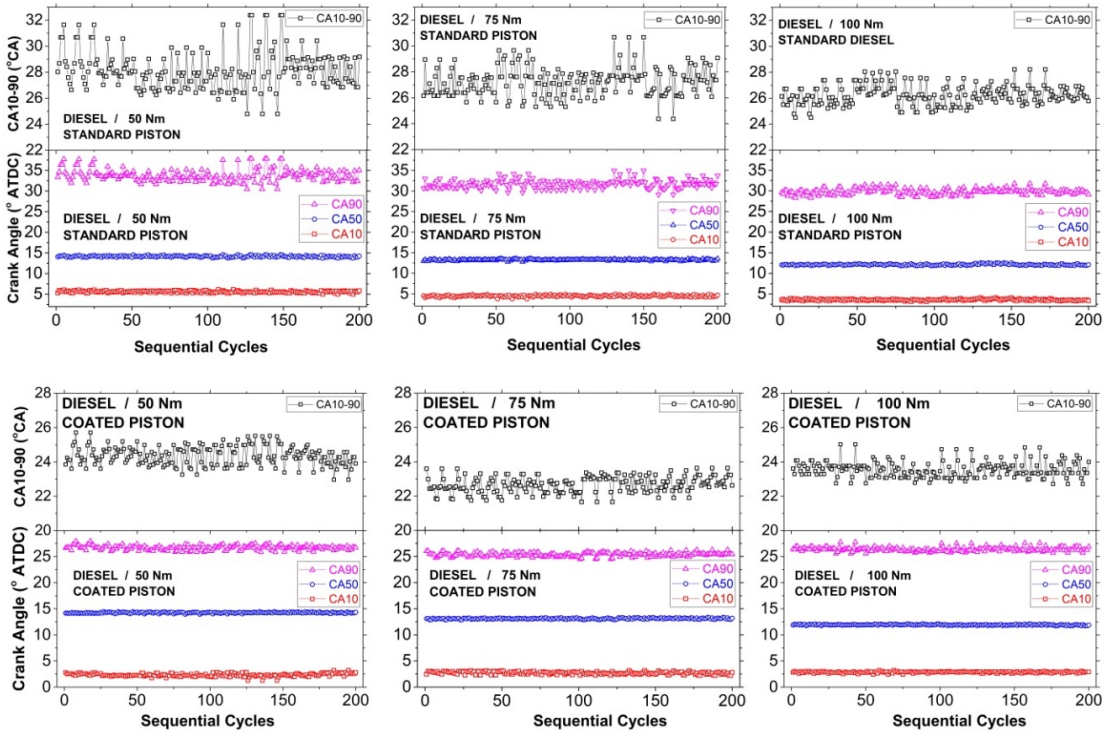

Fig. 11. Cyclic CA10, CA50, CA90, and CA10-90 variations under different loads for diesel mode

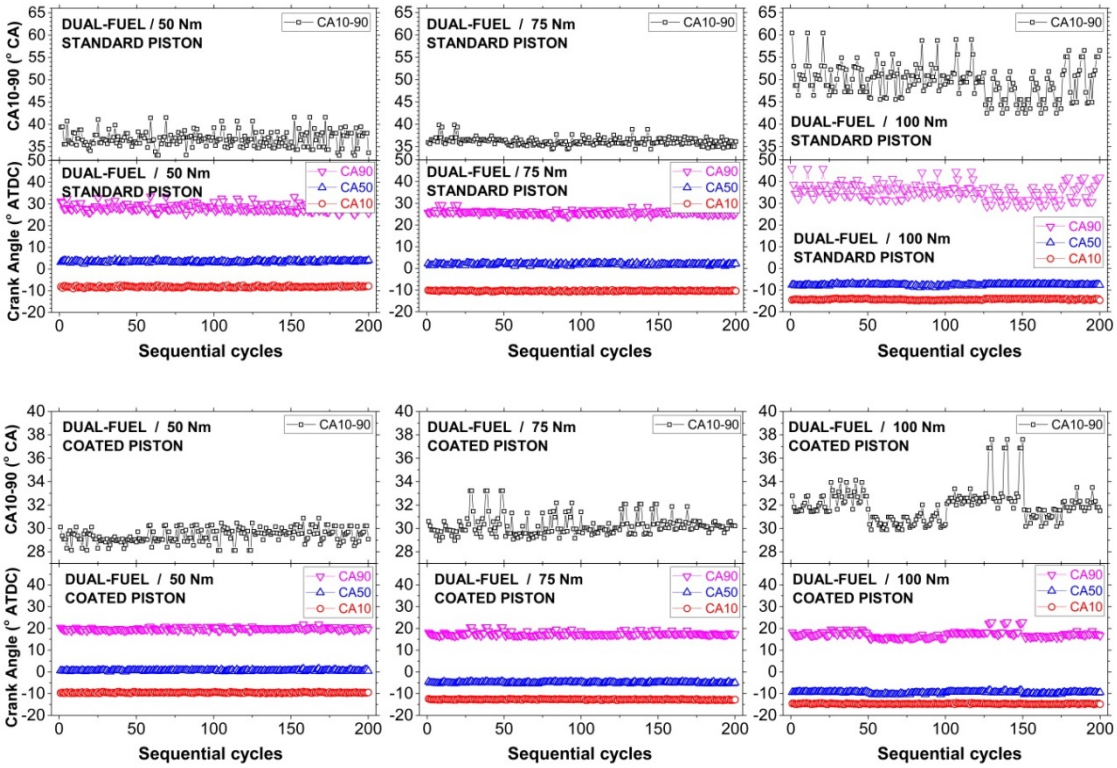

Fig. 12. Cyclic CA10, CA50, CA90, and CA10-90 variations under different loads for dual-fuel mode.

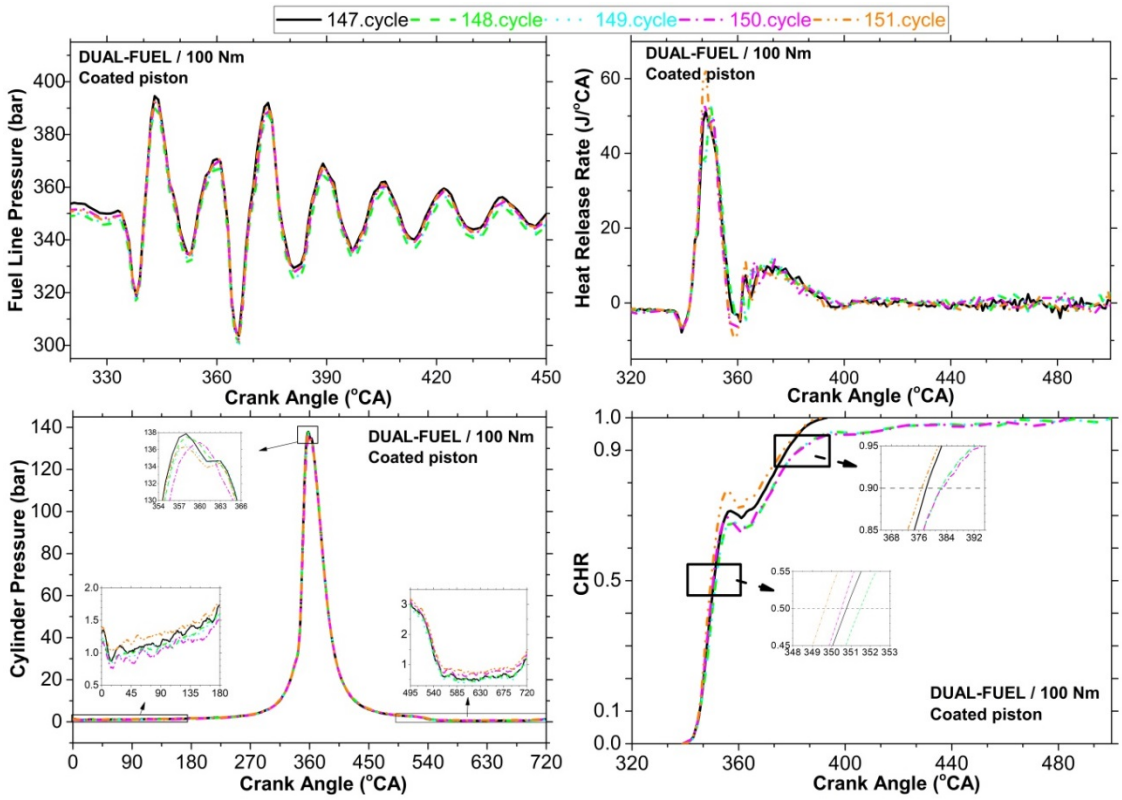

Fig. 13. Cyclic variations in fuel line pressure, heat release rate, cylinder pressure, and CHR for several subsequent cycles.

Corresponding average values of CA10, CA50, CA90 and CA10-90 are presented in Fig. 14a for all test cases. With increasing engine load, average CA10, CA50, and CA90 positions were often advanced and average CA10-90 duration increased that is an expected phenomenon since more fuel is injected in the cylinders with load and needed to more time to burn. On the other hand, it was observed that the piston coating reduced CA10-90

duration. Piston coating leads to higher combustion temperature in the cylinders which in turn encourages flame propagation speed; as a result, time period between CA10 and CA90 is diminished (Venu and Appavu, 2019). Concerning the SD findings of CAs and CA10-90, it could be seen in Fig. 14b that the coated piston was recognizable to lead lower SD, meaning that minimal deviance from the mean value occurred. In case of the single diesel mode with the standard piston operation the highest SD value was obtained with CA90 and CA10-90 duration at 100 Nm as the deviance from the mean value for the CA90 and CA10-90 parameters was highly larger, as clearly seen in Fig. 13.

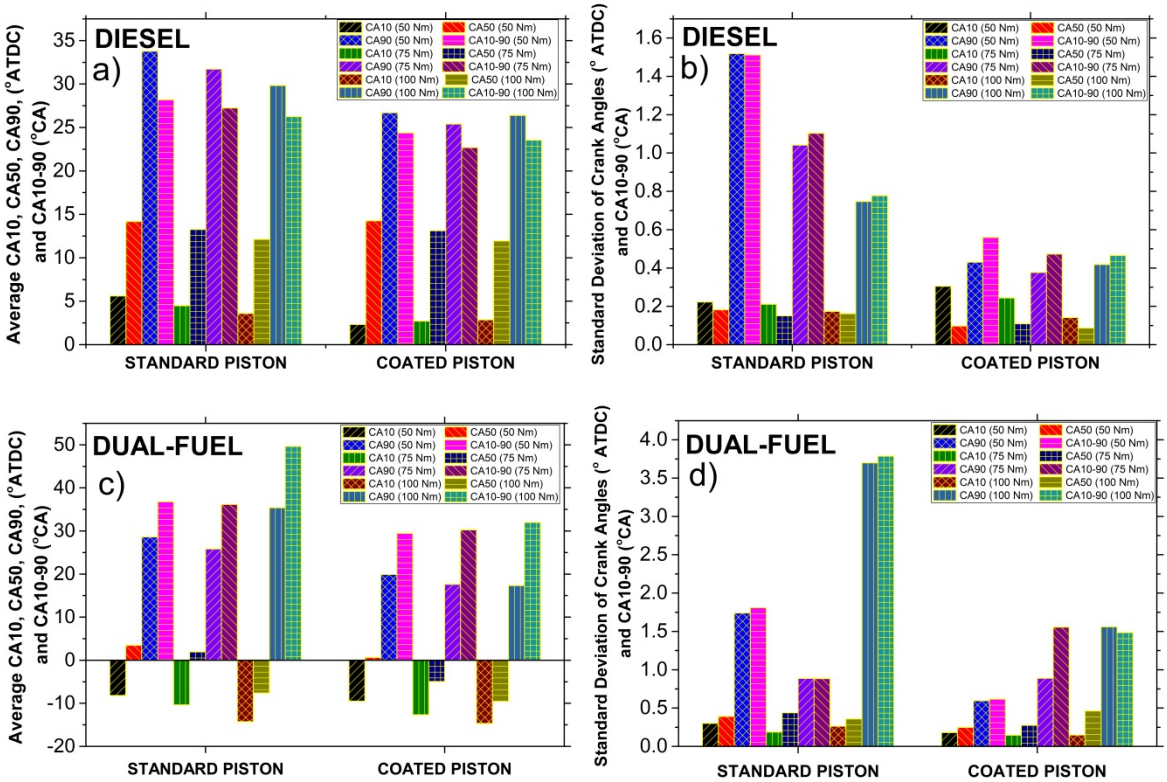

Fig. 14. Average values (a) and SD values (b) of CA10, CA50, CA90 and CA10-90 durations.

Relationship Between Main Combustion Parameters

In Fig.15, it can be seen the relation on fundamental burning parameters covering CP_{max}, PRR_{max}, and IMEP under all the test cases. The highest correlation coefficients were found between CP_{max} and PRR_{max} as R=0.84 and R=0.82 at 50 Nm for dual-fuel operations and R=0.73 and R=0.61 at 100 Nm for diesel operations under the standard and coated pistons, respectively. This represents a strong relation for the mentioned parameters and operating conditions (Şanlı and Yılmaz, 2022). In contrast, the lowest correlation coefficients were found between IMEP and PRR_{max} as 0.02 at 100 Nm for standard piston operation and 0.09 at 75 Nm for coated piston operation under dual-fuel modes, and 0.07 and 0.15 at 75 Nm for standard piston under diesel operations. Except for them, there were not seen higher correlation coefficients but there were mostly weak linear relationships between IMEP and PRR_{max}. As for the correlation between IMEP and CP_{max}, it was found a linear relationship for all dual-fuel modes between IMEP and CP_{max} since the obtained values were in order of R=0.43-0.79. Whereas there were weak linear relationships for single diesel operations, except for the condition of 75 Nm load with the standard piston. Meanwhile, it was generally found poor relationships between each other for the parameters of CA10, CA50, CA90, and CA10-90 at diesel and dual-fuel modes. Also, their relationships with main combustion parameters (CP_{max}, PRR_{max}, and IMEP) were with lower correlation coefficient, suggesting a weak relationship.

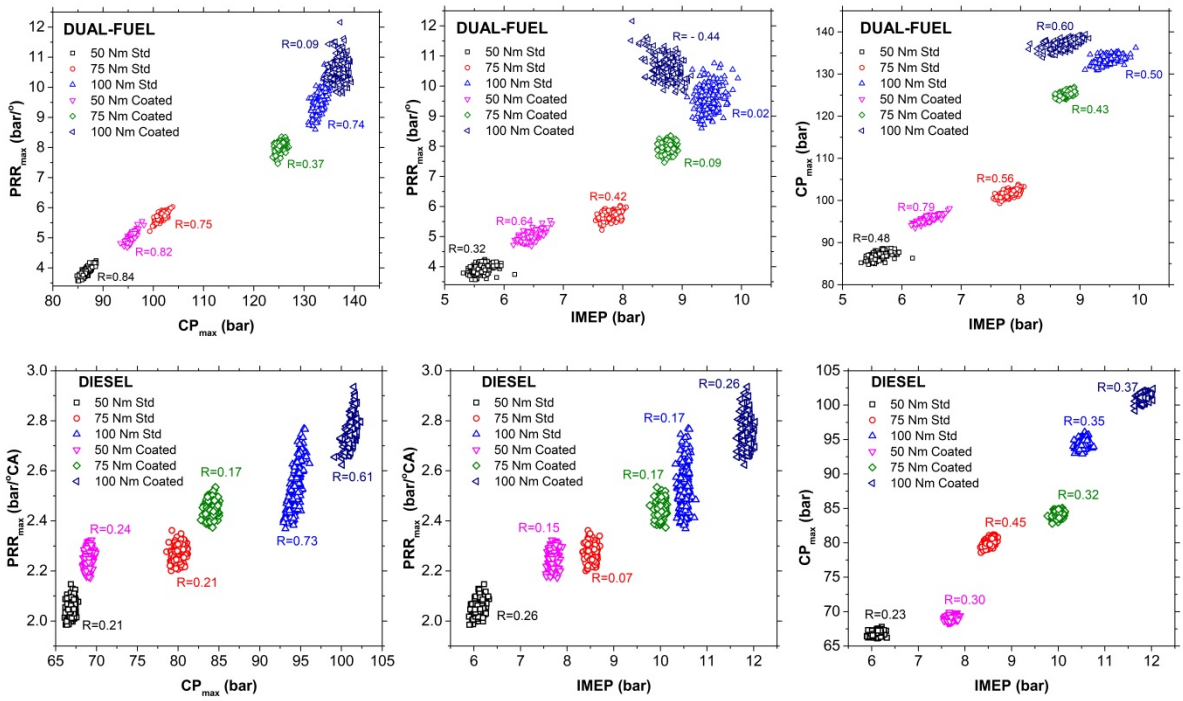

Fig. 15. Correlations between the parameters of CP_{max}, PRR_{max}, and IMEP for dual-fuel operations.

CONCLUSIONS

An experimental study was carried out on the combustion stability of a CRDI automotive diesel engine in which the piston bowls were coated with YSZ at different loads. The study was performed to reveal cyclic variations of main combustion parameters in operation with the gaseous fuels at different loads. Following conclusions were achieved from the study.

-
-
-

Compared to operation with uncoated piston engine, average CP_{max} and PRR_{max} enhanced with coated piston engine for all cycles. As increasing the load, cyclic CP_{max} and PRR_{max} were remarkably advanced and enhanced. Peak value of COV of CP with crank angle decreased under the coated piston engine. At high load of 100 Nm under dual-fuel mode, severe knock indication emerged with coated piston operation, which could be possible reason for higher SD traces of cylinder pressure with the crank angle.

-

IMEP improvement was limited at high load of 100 Nm under coated piston operating due to knock existence. Frequency distribution of cylinder pressure and IMEP showed that the best running was achieved at medium load of 75 Nm. Accordingly, COV and SD results were mostly the best at 75 Nm load for both diesel and gaseous fuel operations under the piston coating.

Cyclic CA10 and CA50 variations were in acceptable range during the cycles. However, CA90 and CA10-90 duration further fluctuated from cycle to cycle. As increasing the engine load, CA90 and CA10-90 fluctuations remarkably reduced in diesel mode but elevated in dual-fuel mode. Furthermore, coating piston reduced cyclic fluctuations of CA90 and CA10-90. In the cyclic discrepancies of CA90 and CA10-90 during sequential cycles, fuel injection pressure and intake air pressure were the critical factors and played an important role.

SD of CA10, CA50, CA90, and CA10-90 was reduced by the coated piston under diesel and dual-fuel modes.

Relationship between main combustion characteristics varied with given operation cases. Correlation coefficient between IMEP-CP_{max} parameters was always higher than 0.4, meaning that there was a linear relationship and in acceptable range for all operation cases. The highest correlation coefficient was found between PRR_{max} and CP_{max} parameters, which are 0.84 and 0.82 corresponding to low load of 50 Nm load under dual-fuel mode with coated and uncoated pistons, respectively.

In the future studies, it is recommended that a more comprehensive study is conducted with another alternative fuels, such as natural gas, biogas, biodiesel, higher alcohols. Furthermore, tested engine parameters can be expanded with more range of loads, speeds, and fuel fractions.

REFERENCES

Adomeit P., Lang O., Pishinger S., Aymanns R., Graf M., Stapf G., 2007, Analysis of cyclic fluctuations of charge motion and mixture formation in a DISI engine in stratified operation, *SAE Technical Paper,* 2007-01-1412.

Ali H.L., Li F., Wang Z., Shuai S., 2018, Effect of ceramic coated pistons on the performance of a compressed natural gas engine, *IOP conference series: Materials Science and Engineering*, 417, 012021.

Assanis D., Wiese K., Schwarz E., Bryzik W., 1991, The effects of ceramic coatings on diesel engine performance and exhaust emissions, *SAE Technical Paper,* 910460.

Aydin H., 2013, Combined effects of thermal barrier coating and blending with diesel fuel on usability of vegetable oils in diesel engines, *Applied Thermal Engineering*, 2013;51(1-2):623-9.

Aydın S., Sayin C., Aydin H., 2015, Investigation of the usability of biodiesel obtained from residual frying oil in a diesel engine with thermal barrier coating, *Applied Thermal Engineering*, 80, 212-9.

Barton R., Kenemuth D., Lestz S., Meyer W, 1970, Cycle-by-cycle variations of a spark ignition engine- A statistical analysis, *SAE Technical Paper,* 700488.

Bouguessa R., Tarabet L., Loubar K., Bilmrabet T., Tazerout M., 2020, Experimental investigation on biogas enrichment with hydrogen for improving the combustion in diesel engine operating under dual fuel mode, *International Journal of Hydrogen Energy*, 45(15), 9052 – 63.

Caputo S., Millo F., Boccardo G., Piano A., Cifali G., Pesce F.C., 2019, Numerical and experimental investigation of a piston thermal barrier coating for an automotive diesel engine application. *Applied Thermal Engineering*, 162, 114233.

Cerit M. and Coban M., 2014, Temperature and thermal stress analyses of a ceramic-coated aluminum alloy piston used in a diesel engine, *International Journal of Thermal Sciences*, 77, 11-8.

Chen Z., He J., Chen H., Geng L., Zhang P., 2021, Experimental study on cycle-to-cycle variations in natural gas/methanol bi-fueled engine under excess air/fuel ratio at 1.6, *Energy*, 224, 120233.

Civiniz M., Hasimoğlu C., Şahin F., Salman M.S., 2008, Impact of thermal barrier coating application on the performance and emissions of a turbocharged diesel engine, *Proc IMechE Part D: J Automobile Engineering*, 222(12), 2447-55.

Godiganur V.S., Nayaka S., Kumar G.N., 2021, Thermal barrier coating for diesel engine application – A review. *Materials Today: Proceedings,* 45,133-7.

Goud G.B., Singh C.T.D.K., 2015, Investigation of CI diesel engine emission control and performance parameters using biodiesel with YSZ coated piston crown. *International Journal of Engineering and Technology*, 2(3), 467-74.

Gupta S.K. and Mittal M., 2019, Effect of compression ratio on the performance and emission characteristics, and cycle-to-cycle combustion variations of a spark-ignition engine fueled with bio-methane surrogate, *Applied Thermal Engineering*, 148, 1440-53.

Hazar H., 2010, Cotton methyl ester usage in a diesel engine equipped with insulated combustion chamber, *Applied Energy*, 87,134-40.

Hazar H., Ozturk U., Gül H., 2016, Characterization and effect of using peanut seed oil methyl ester as a fuel in a low heat rejection diesel engine, *Energy&Fuels,* 30(10), 8425-31.

Heywowski T., Weronski A., The effect of thermal barrier coatings on diesel engine performance, *Vacuum,* 65, 427-32.

Kyrtatos P., Brücker C., Bouchoulos K., 2016, Cycle-to-cycle variations in diesel engines, *Applied Energy,* 171, 120-32.

Lawrence P., Mathews P.K., Deepanraj B., 2011, Experimental investigation on performance and emission characteristics of low heat rejection diesel engine with ethanol as fuel, *American Journal of Applied Sciences*, 8(4), 348-54.

Liu J.J., Ding S.F., Ding S.L., Gao J.S., Song E.Z., Yang F.Y., 2022, Effects of gas injection timing on combustion instability for a spark ignition natural gas engine under low load, *Applied Thermal Engineering,* 206, 118144.

Özer S., Vural E., Özel S., 2021, Effects of fusel oil use in a thermal coated engine, *Fuel*, 306, 121716.

Pera C., Chevillard S., Reveillon J.,2013, Effects of residual burnt gas heterogeneity on early flame propagation and on cyclic variability in spark-ignited engines, *Combustion and Flame*, 160(6), 1020-32.

Ramasamy N., Kalam M.A., Varman M., Teoh Y.H., 2021, Comparative studies of piston crown coating with YSZ and $AL_2O_3.SiO_2$ on engine out responses using conventional diesel and palm oil biodiesel, *Coatings,* 11(8), 885.

Ramu P., Saravanan C.G.,2009, Effect of ZrO2-Al2O3 and SiC coating on diesel engine to study the combustion and emission characteristics, *SAE Technical Paper,* 2009-01-1435.

Ramu P., Saravanan C.G., 2009, Investigation of combustion and emission characteristics of a diesel engine with oxygenated fuels and thermal barrier coating, *Energy&Fuels*, 23(2), 653-6.

Reddy G.V., Krupakaran R.L., Tarigonda H., Reddy A.R., Rasu N.G., 2021, Energy balance and emission analysis on diesel engine using different thermal barrier

coated pistons. *Materials Today: Proceedings,* 43(1), 646-54.

Schulz U., Leyens C., Fritscher K., Peters M., Saruhan-Brings B., Lavigne O., Dorvaux J.M., Poulain M., Mevrel R., Caliez M., 2003, Some recent trends in research and technology of advanced thermal barrier coatings. *Aero Science and Technology,* 7, 73-80.

Selvam M., Shanmugan S., Palani S., 2018, Performance analysis of IC engine with ceramic-coated piston. *Environmental Science and Pollution Research*, 25, 35210-20.

Serrano J.R., Arnau F.J., Martin J., Hernandez M., Lombard B., 2015, Analysis of engine walls thermal insulation: Performance and Emissions, *SAE Technical Paper*, 2015-01-1660.

Shabir M.F., Prasath B.R., Tamilporai P., 2014, Analysis of combustion performance and emission of extended cycle and iEGR for low heat rejection turbocharged direct injection diesel engines, *Thermal Science*, 18(1), 129-42.

Sivakumar G. and Kumar S.S., 2014, Investigation on effect of Yttria Stabilized Zirconia coated piston crown on performance and emission characteristics of a diesel engine, *Alexandria Engineering Journal,* 53(4), 787-94.

Şanlı A., Yılmaz I.T., Gümüş M., 2019, Experimental evaluation of performance and combustion characteristics in a hydrogen-methane port fueled diesel engine at different compression ratios. *Energy&Fuels*, 34, 2272-83.

Şanlı A., Yılmaz I.T., 2022, Cycle-to-cycle combustion analysis in hydrogen fumigated common-rail diesel engine. *Fuel*, 320, 123887.

Şanlı A., 2023, Experimental study of combustion and cyclic variations in a CRDI engine fueled with heptanol/iso-propanol/butanol and diesel blends. *Energy*, 269, 126800.

Taymaz I., 2007, The effect of thermal barrier coatings on diesel engine performance. *Surface and Coatings Technology*, 201(9-11), 5249-52.

Venu H. and Appavu P., 2019, Analysis on a thermal barrier coated (TBC) piston in a single cylinder diesel engine powered by Jatropha biodiesel-diesel blends, *SN Applied Science*, 1,1669.

Vittal M., Borek J.A., Marks D.A., Boehman A.L., Okrent D.A., Bentz A.P., 1999, The effects of thermal barrier coatings on diesel engine emissions, *J. Eng Gas Turbines Power,* 121(2), 218-25.

Wang Y., Xiao F., Zhao Y., Li D., Lei X., 2015, Study on cycle-by-cycle variations in a diesel engine with dimethyl ether as port premixing fuel, *Applied Energy*, 143, 58-70.

Wang Y., Ma T., Liu L., Yao M., 2021, Numerical investigation of the effect of thermal barrier coating on combustion and emissions in a diesel engine, *Applied Thermal Engineering*, 2021, 186, 116497.

Yao M., Ma T., Wang H., Zheng Z., Liu H., Zhang Y. A., 2018, Theoretical study on the effects of thermal barrier coating on diesel engine combustion and emission characteristics, *Energy*, 162, 744-52.

Zhong L., Singh I.P., Han J., Lai M-C., Henein N.A., Bryzik W., 2003, Effect of cycle-to-cycle variation in the injection pressure in a common rail diesel injection system on engine performance. *SAE Technical Paper*, 2003-01-0699.